Published OnlineFirst April 13, 2016; DOI: 10.1158/0008-5472.CAN-16-0316

Integrated Systems and Technologies

Cancer Research

Identification of MYC-Dependent Transcriptional Programs in Oncogene-Addicted Liver Tumors

Theresia R. Kress[1,2], Paola Pellanda[1], Luca Pellegrinet[3], Valerio Bianchi[1], Paola Nicoli[2], Mirko Doni[2], Camilla Recordati[4], Salvatore Bianchi[1], Luca Rotta[2], Thelma Capra[2], Micol Ravà[1,2], Alessandro Verrecchia[2], Enrico Radaelli[5], Trevor D. Littlewood[3], Gerard I. Evan[3], and Bruno Amati[1,2]

Abstract

Tumors driven by activation of the transcription factor MYC generally show oncogene addiction. However, the gene expression programs that depend upon sustained MYC activity remain unknown. In this study, we employed a mouse model of liver carcinoma driven by a reversible tet-MYC transgene, combined with chromatin immunoprecipitation and gene expression profiling to identify MYC-dependent regulatory events. As previously reported, MYC-expressing mice exhibited hepatoblastoma- and hepatocellular carcinoma–like tumors, which regressed when MYC expression was suppressed. We further show that cellular transformation, and thus initiation of liver tumorigenesis, were impaired in mice harboring a MYC mutant unable to associate with the corepressor protein MIZ1 (*ZBTB17*). Notably, switching off the oncogene in advanced carcinomas revealed that MYC was required for the continuous activation and repression of distinct sets of genes, constituting no more than half of all genes deregulated during tumor progression and an even smaller subset of all MYC-bound genes. Altogether, our data provide the first detailed analysis of a MYC-dependent transcriptional program in a fully developed carcinoma and offer a guide to identifying the critical effectors contributing to MYC-driven tumor maintenance. *Cancer Res; 76(12); 3463–72. ©2016 AACR.*

Introduction

Overexpression of the oncogenic transcription factor MYC is frequently observed in human tumors (1), and analysis of multiple mouse models confirmed MYC's fundamental impact on tumorigenesis and tumor maintenance (2). MYC belongs to the bHLH-LZ (basic helix-loop-helix leucine zipper) transcription factor family and dimerizes with the bHLH-LZ partner Max to bind DNA, with a preference for the E-box motif CACGTG, or variants thereof. In cells, however, MYC interacts very promiscuously with chromatin: if expressed at high enough levels, it can be detected at virtually all active regulatory elements in the genome, including promoters and distal enhancers, a phenomenon dubbed "invasion" (3–8). Even in this setting, however, MYC acts to up- and downregulate defined subsets of all targeted loci (5, 6, 8), its mere binding at any given locus being insufficient to predict gene regulation (reviewed in ref. 8). Altogether, the principles underlying the specificity of MYC-driven transcriptional responses remain largely unknown, and are likely to include cell-, context- or promoter-dependent cues (9, 10).

Cellular transformation by MYC requires not only dimerization with Max and DNA binding, mediated by its C-terminal bHLH-LZ domain (11), but also the integrity of its N-terminal region, which includes its transactivation domain (12). Through this region, MYC can associate with a wide range of coregulatory proteins and complexes, including histone modifiers, chromatin remodelers, or regulators of RNA polymerase II (RNAPII) processivity, such as the kinase complexes TFIIH and pTEF-B (13). Hence, MYC is most likely to activate gene expression at multiple levels, including RNAPII loading and elongation (14, 15), as well as to impact cotranscriptional events such as mRNA capping (16). Transcriptional repression by MYC remains to be understood mechanistically, but requires the same N- and C-terminal terminal domains of the protein (17). The best-characterized MYC cofactor in this process is MIZ1, a zinc-finger protein involved in the regulation of a large fraction (up to 40%) of MYC-repressed genes (6, 18). The use of a MYC mutant specifically impaired in MIZ1 binding (V394D, hereafter MYC-VD) revealed an important role for this interaction in tumorigenesis, in particular, in the thymus (19) and medulloblastoma (20). Hence, albeit the regulatory programs involved in each particular tumor type remain to be fully characterized, activation and repression of transcription by MYC are both likely to contribute to its oncogenic function.

Over the last two decades, numerous studies have aimed at profiling MYC-driven transcriptional programs, whether in cell

[1]Center for Genomic Science of IIT@SEMM, Fondazione Istituto Italiano di Tecnologia (IIT), Milan, Italy. [2]Department of Experimental Oncology, European Institute of Oncology (IEO), Milan, Italy. [3]Department of Biochemistry, University of Cambridge, Downing Site, Cambridge, United Kingdom. [4]Mouse & Animal Pathology Laboratory, Fondazione Filarete, Milan, Italy. [5]VIB11 Center for the Biology of Disease, KU Leuven Center for Human Genetics, KU Leuven, Leuven, Belgium.

Note: Supplementary data for this article are available at Cancer Research Online (http://cancerres.aacrjournals.org/).

Current address for V. Bianchi: Hubrecht Institute-KNAW & University Medical Center Utrecht, Uppsalalaan 8, Utrecht 3584 CT, the Netherlands.

Corresponding Author: Bruno Amati, Center for Genomic Science of IIT@SEMM, Fondazione Istituto Italiano di Tecnologia (IIT), Via Adamello 16, Milan 20139, Italy. Phone: 39-02-5748-9824; Fax: 39-02-9437-5990; E-mail: bruno.amati@iit.it

doi: 10.1158/0008-5472.CAN-16-0316

Published OnlineFirst April 13, 2016; DOI: 10.1158/0008-5472.CAN-16-0316

lines or tumor models. In line with its biologic roles in either normal or tumor cells, MYC has emerged as a central regulator of growth-promoting processes, such as DNA replication, energy production, ribosomal biogenesis, glucose and glutamine metabolism, the biosynthesis of amino acids and nucleotides, and others (8, 10, 21). Nonetheless, because of the aforementioned limitations in discriminating functional from incidental DNA-binding events *in vivo* (8), we are still lacking definitive identification of the genes that are directly regulated by MYC in tumor progression and/or maintenance.

Here, we combined a LAPtTA transgene expressing a tetracycline-controlled transactivator (tTA) in the liver, with either of two tTA-regulated c-*MYC* transgenes, one encoding wild-type MYC, the other MYC-VD (19). Analogous to previous studies based on a different transgenic founder (22, 23), MYC-expressing mice developed oncogene-addicted liver tumors that rapidly regressed upon silencing of MYC expression by doxycycline. Expression profiling in developing and regressing tumors allowed us to discriminate secondary from primary, MYC-dependent regulatory events, the latter including equivalent numbers (ca. 1,200-1,400) of MYC-induced and repressed genes. As in other tissues (19, 24), MYC-VD showed reduced tumorigenic potential relative to wild-type MYC in the liver, owing to an essential role of the MYC/MIZ1 interaction in repression in tumor initiation.

Materials and Methods

Cell culture

Embryonal liver cells BNL CL.2 (ATCC TIB-73) and $3T9^{fl/fl}$ fibroblasts (25, 26) were cultured in DMEM, supplemented with 10% FBS, 2 mmol/L L-glutamine, and penicillin/streptomycin. Primary fetal hepatoblasts (fHB) and immortalized lines from C57/JHsd mice were purified (as described below) on embryonic day E18.5 and cultured in DMEM supplemented with 10% FBS, 2 mmol/L L-glutamine, and penicillin/streptomycin as well as HGF (40 ng/mL, Peprotech), EGF (20 ng/mL, Peprotech), and dexamethasone (1 mmol/L, Sigma). On day 3 after purification, fHBs were infected with retroviruses encoding sh*p53* or human MYC or MYC-VD. Upon immortalization, cells were plated on regular culture plates in growth medium lacking additional growth factors. Super-infection with RAS^{G12V} was performed after immortalization.

For 5'-Bromo-2'Deoxyuridine (BrdUrd) stainings, $3T9^{fl/fl}$ fibroblasts were incubated for 15 minutes with 33 μmol/L of BrdUrd (B9285, Sigma), fixed, stained with antibodies targeting BrdUrd (347580, Becton Dickinson), and FITC-conjugated donkey-anti-mouse antibodies (715-095-150, Jackson Immuno Research). Fluorescence signal intensity was acquired with a FACSCalibur (BD Biosciences) and analyzed using the FlowJo software.

Cre-mediated deletion of the floxed *c-MYC* alleles in $3T9^{fl/fl}$ fibroblasts was achieved by addition of 100 μg/mL of Tat-cre to the culture medium (supplemented with 0.1% serum). After incubation at 37°C for 1 hour, 0.1 mmol/L of chloroquine (Sigma) was added to the medium for an additional 1 hour. Cells were washed with PBS and regular culture medium was added for further cultivation.

Animal experiments

FVB mice transgenic for tet-MYC (termed TetO-Myc in the original publication) were kindly provided by Martin Eilers (Theodor Boveri Institute, Würzburg, Germany; ref. 19). In a model of T-cell lymphomagenesis, several tet-MYC-WT and V394D (hereafter VD) founder lines have been tested (see Supplementary Fig. S2A in ref. 19). In our study, we used the founder line MYC-wt-1 (#3584) for tet-MYC-WT and MYC-VD-2 (#3557) for tet-MYC-VD. LAPtTA transgenic mice on C57/Bl6 background [B6.Cg-Tg(tTALap)5Bjd/J; Jackson laboratories] were subjected to accelerated backcrossing into the FVB strain for at least 5 passages until > 98.6% clean FVB background was reached. Double-transgenic offsprings (heterozygous for either transgene) were monitored 3 times per week for tumor development. Mice were sacrificed and scored for survival curves when moribund. Tumor nodules or control liver tissue from age-matched littermates were dissected and processed freshly or frozen and stored at −80°C until further analysis. To switch of transgene expression, doxycycline was administered in the food *ad libitum* (Mucedola). To avoid effects of the circadian rhythm on gene expression and DNA binding, samples were taken at the same time of the day (between 10 and 12 am). Experiments involving animals were done in accordance with the Italian Laws (D.lgs. 26/2014), which enforces Dir. 2010/63/EU (Directive 2010/63/EU of the European Parliament and of the Council of 22 September 2010 on the protection of animals used for scientific purposes).

Computational analysis

Computational analyses of next-generation sequencing (NGS) data were performed as described elsewhere (5), with few modifications mentioned below. Briefly, ChIP-seq and RNA-seq libraries were sequenced with the Illumina HiSeq 2000 to a read length of 50 bp (ChIP-seq: single-end, RNA-seq: paired-end). Reads were filtered using the FASTX-Toolkit suite (http://hannonlab.cshl.edu/fastx_toolkit/) and the read quality was assessed using the FastQC application (www.bioinformatics.babraham.ac.uk/projects/fastqc). After removal of duplicated reads, unique ones were mapped to the mouse refseq genome mm9.

ChIP-seq reads were aligned using the BWA aligner using default settings. Peaks were called with the MACS2 software, retaining only peaks with a $P<1e{-}5$ (narrow peaks, such as MYC) or $<1e{-}8$ (broad peaks, such as RNA Pol II, H3K4me3, H3K27ac). Enrichment values were determined as $\log2(ChIP_{nrc} - Input_{nrc})$, where $ChIP_{nrc}$ and $Input_{nrc}$ are the normalized read counts (nrc) in the regions of interest in the ChIP and in the corresponding input sample.

RNA-seq reads were aligned with the TopHat aligner with default parameters. Read counts were associated to exons using the HTSeq software (http://www-huber.embl.de/users/anders/HTSeq/doc/overview.html). The expression of a gene with more than one isoform was determined as the mean of the expression values across all of its isoforms. The expression of each transcript was estimated as RPKM value (reads per kilobase per million mapped exonic reads), defined over exons alone. Differentially expressed genes (DEG) were identified using the Bioconductor package DESeq2. DEGs in this study were defined as genes whose associated *q* value (from the DESeq2 output) was lower than 0.01 and whole log2 fold change was >1 or <(−1). We considered only protein-coding genes and considered them expressed if the RPKM value was above 3 (average of biologic replicates) in at least one experimental condition. As experimental conditions, we considered control liver (C), tet-MYC tumors before (T) or after (Toff) short-term tet-MYC inactivation, or tet-MYC V394D tumors (Tvd). This cut-off parameter resulted in approximately 11,900 expressed genes.

Published OnlineFirst April 13, 2016; DOI: 10.1158/0008-5472.CAN-16-0316

Immunohistochemistry

Tissue was washed in PBS, fixed in 4% (v/v) of paraformaldehyde at room temperature for at least 6 hours, washed in PBS, and then stored in 70% EtOH at 4°C until further processing. Tissue was dehydrated with increasing concentrations of EtOH, embedded in paraffin blocks, cut into 5-μm sections and mounted on glass slides. Sections were dewaxed and rehydrated through an ethanol scale, heated in citrate solution (BioGenex #HK086-9K) in a water bath at 99°C for 30 minutes for antigen unmasking, washed once in water, and treated with 3% H_2O_2 for quenching of endogenous peroxidases. Tissue sections were stained with the following antibodies: MYC (Y69; Abcam, ab32072; 1:100) or E-cadherin (ECCD-1; Life Technologies, 131800; 1:200). After incubation with with primary antibodies, slides were washed twice with TBS and then incubated with secondary antibodies (Dako Cytomation Envision System Labelled Polymer-HRP) for 45 minutes. The signal was revealed with DAB peroxidase substrate solution (Dako) for 2 to 10 minutes. Slides were finally counterstained with hematoxylin, dehydrated through alcoholic scale, and mounted with Eukitt (Bio-Optica). Images were acquired with the Olympus BX51 upright microscope (software NIS, Nikon).

Data availability and additional methods

ChIP-seq and RNAseq data have been submitted to the NCBI GEO database with the accession number GSE76078. Further methods can be found in Supplementary Information.

Results

Induction of hepatoblastomas and HCC-like tumors by MYC

To study the interplay between MYC activity, transcription, and chromatin organization in liver tumors, we used a tet-MYC/LAPtTA mouse model as originally described (Supplementary Fig. S1A; refs. 22, 23) but based on two different c-*MYC* transgenes, tet-MYC-WT and tet-MYC-VD, the latter expressing the MYC V394D mutant defective in MIZ1 binding (19). As expected, breeding of either of these tet-MYC strains with LAPtTA animals in the absence of doxycycline led to expression of the human c-*MYC* mRNA in liver progenitor cells *in utero* in double-transgenic embryos (Supplementary Fig. S1B).

We first characterized tumor progression induced by wild-type MYC: at embryonic day E18.5, double-transgenic tet-MYC-WT/LAPtTA (dtg) embryos appeared phenotypically indistinguishable from control siblings (Supplementary Fig. S1C), retained a normal liver architecture at the histologic level (data not shown), but showed slightly increased liver sizes (Supplementary Fig. S1D and S1E). By 6 weeks of age, tet-MYC-WT/LAPtTA mice showed a gross increase in abdominal size and fully penetrant, gender-independent development of multinodal liver tumors that expressed high MYC levels (Fig. 1A–E and Supplementary Fig. S1F). Closer histologic assessment revealed both epithelial hepatoblastoma and HCC-like tumors, confirming previous observations (23, 27). Tumors stained positive for E-cadherin (Fig. 1E) expressed mRNAs encoding markers of fetal progenitor cells, such as *Afp*, *Dlk1*, *Sall4* (Supplementary Fig. S1H), and contained frequent mitotic and apoptotic cells (Supplementary Fig. S1G). As previously reported, MYC-driven liver tumors showed full oncogene addiction (23), as feeding tumor-bearing mice with doxycycline-containing food rapidly suppressed MYC expression (Fig. 1F) and induced tumor regression, with significant decreases in tumor mass within a week, and apparently normal livers and healthy conditions within 3–4 weeks (Fig. 1G). In summary, tet-MYC activation *in utero* caused a prenatal increase in liver size and the fully penetrant development of MYC-dependent hepatoblastomas by the age of 4–6 weeks.

On the basis of a distinct tet-MYC strain, but the same LAPtTA transgene and experimental scheme used here, others reported slower tumor development following MYC activation *in utero* (22). The reasons for these differences may be partly genetic (distinct *MYC* transgenes), partly environmental, but are beyond the scope of this study.

MYC-induced liver tumorigenesis is impaired by the V394D mutation

We then addressed whether the V394D mutation affected MYC's oncogenic activity in the liver, as previously reported in lymphomas (19). Relative to tet-MYC-WT, tet-MYC-VD animals showed delayed tumorigenesis (Fig. 1B). Once formed, however, MYC-WT- and MYC-VD–induced tumors appeared equally aggressive, moribund animals showing comparable liver weights (Fig. 1H) and tumor load (Supplementary Fig. S2A). Albeit variable among individual tumors, wild-type and mutant MYC were expressed within similar ranges, either as mRNA (Fig. 1I) or protein (Supplementary Fig. S2B). As with MYC-WT, MYC-VD–induced tumors showed no significant gender differences (Supplementary Fig. S2C) and expressed the fHB markers *Afp*, *Dlk1*, *Sall4* (Supplementary Fig. S2E) and E-cadherin (Fig. 1E). By histologic analysis, MYC-VD showed the same tumor types as MYC-WT, albeit with increased frequency of the HCC-like tumors compared with hepatoblastoma (Supplementary Fig. S2E). As a marker of apoptosis, we monitored PARP cleavage, revealing variability among tumors, but no significant difference between the two *MYC* genotypes (Supplementary Fig. S2B).

To address MYC function at a pretumoral stage, we purified LAPtTA/tet-MYC-WT and VD fHBs by magnetic cell sorting with an E-cadherin antibody (28). RT-PCR analysis revealed similar *MYC* mRNA levels in both populations (Supplementary Fig. S1B), showing comparable activation of a MYC-induced gene (*Smpdl3b*) but defective repression of *Cdkn1a* by MYC-VD, as expected (Supplementary Fig. S2F; ref. 29). MYC-WT and MYC-VD led to similar increases in the number of fetal hepatoblasts recovered per embryo (Supplementary Fig. S2G), suggesting equivalent proliferative activities. Both forms of MYC also rescued cell proliferation in mouse 3T9 fibroblasts upon deletion of the endogenous c-*MYC* gene (25), as shown by cell counting, BrdUrd incorporation, and colony formation (Supplementary Fig. S3A–S3C), confirming that MYC-VD possesses an intact proliferative ability.

To further confront the oncogenic potential of wild-type and mutant MYC, we purified wild-type E18.5 hepatoblasts and infected these cells with retroviruses expressing MYC-WT or MYC-VD together with an shRNA targeting *TP53*, allowing us to obtain immortalized cell lines that could be further transformed by expression of oncogenic RAS^{G12V} (28). RAS^{G12V} was expressed at similar levels and enhanced proliferation of cells with either MYC-WT or MYC-VD (Supplementary Fig. S3D and S3E) but the latter showed marked defects in cellular transformation, as assayed either *in vitro* by sphere formation in methylcellulose (Fig. 1J) or *in vivo* by subcutaneous tumor growth in CD1-nude mice (Fig. 1K). We also expressed tamoxifen-responsive MYC-ER^{TAM} chimeras in the murine fetal liver progenitor cell line BNL

Published OnlineFirst April 13, 2016; DOI: 10.1158/0008-5472.CAN-16-0316

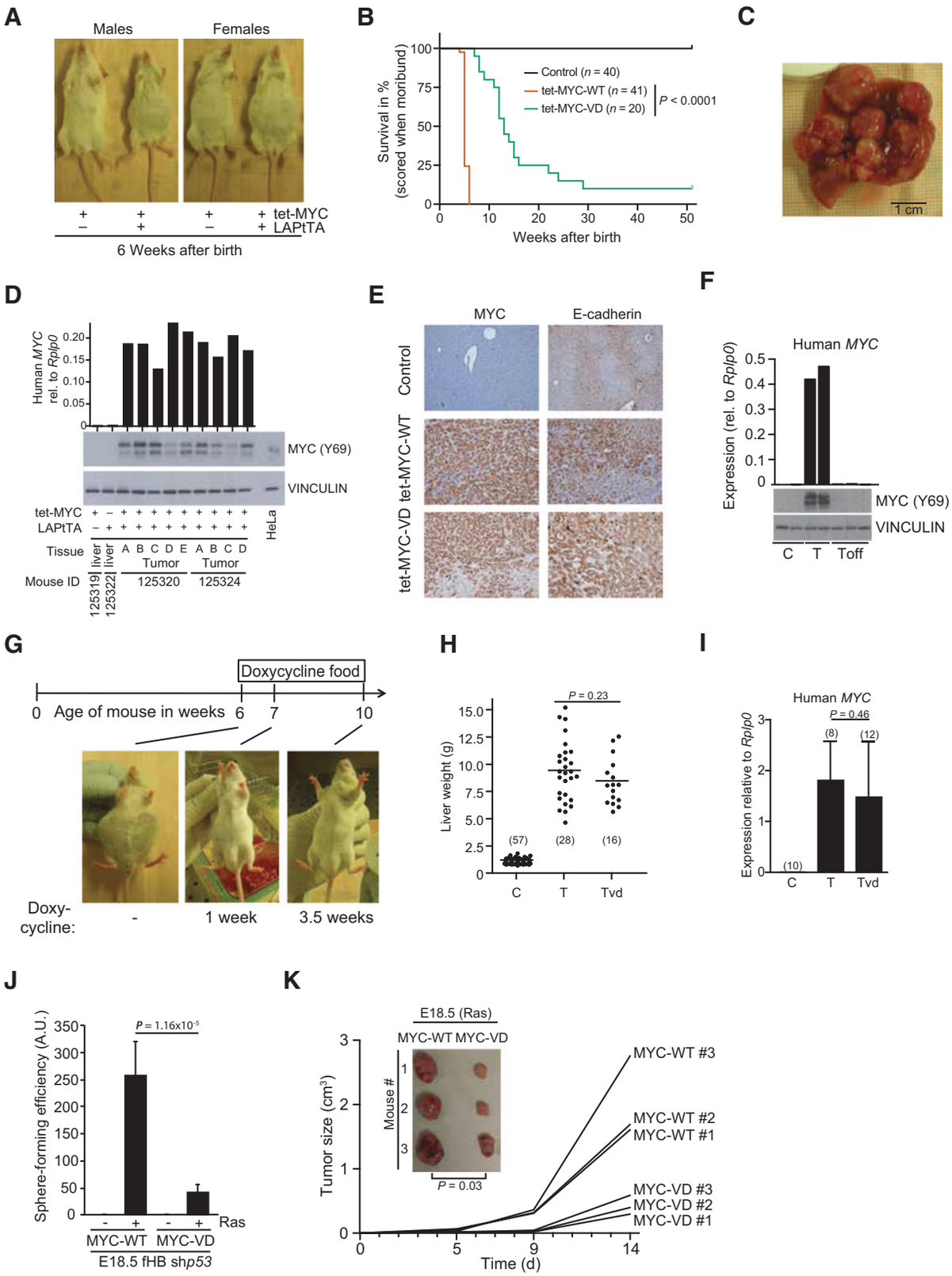

Published OnlineFirst April 13, 2016; DOI: 10.1158/0008-5472.CAN-16-0316

CL.2: again, activation of either the WT or VD forms of MYC-ER^{TAM} caused a similar increase in proliferative potential (Supplementary Fig. S3F). When cultured in semi-solid medium, however, cells expressing the MYC-ER VD mutant showed a marked decrease in sphere-forming ability relative to the MYC-ER WT controls (Supplementary Fig. S3F). Remarkably, knockdown of MIZ1 with either of two different shRNAs (#8 and #9) decreased sphere-forming efficiency of MYC-ER WT to levels comparable with those of MYC-ER VD, ablating the difference between the two forms of MYC. Hence, the deficit in cellular transformation of VD mutant was entirely attributable to its interaction with MIZ1 (29). Taken together, the above data indicate that while retaining normal proliferative activity, MYC-VD is defective in cellular transformation, affecting most likely the frequency of tumor initiation *in vivo*.

Short-term MYC inactivation in tumors allows distinction between MYC-dependent and independent genes

When comparing transcriptome profiles at steady state in control and tumor tissue, changes in any given mRNA may follow either from its direct transcriptional control by MYC, or from indirect regulatory effects. To discriminate between those two scenarios, we took advantage of our switchable model and determined RNA-seq profiles in three conditions: control livers (C), tet-MYC-WT–induced tumor nodules (T), and tumors 16 hours after tet-MYC-WT shutdown by exposure to doxycycline-containing food (Toff). Hierarchical clustering of RNA-seq data clearly separated the three conditions, while samples within each group showed strong correlations (Fig. 2A and B; Supplementary Table S1). As expected, gene expression changes between the two main transitions, C→T and T→Toff, were counter-correlated at the genome-wide level (Supplementary Fig. S4A). However, Toff showed only a partial recovery of the C pattern, remaining closer to T than to C (Fig. 2A–C). Calling for differentially expressed genes (DEG, Supplementary Fig. S4B; Supplementary Table S1) revealed that most of the MYC-dependent genes in tumors (i.e., DEG in T→Toff) also scored during tumorigenesis (C→T), although larger numbers of DEGs in C→T showed no MYC dependency in T→Toff (Fig 2C–E). In this setting, MYC-dependent mRNAs most likely represented directly regulated, primary target genes, whereas MYC-independent genes were most likely deregulated in tumors via secondary mechanisms. Most importantly, the distinction between these two regulatory categories was not a trivial consequence of differences in either expression levels (Fig. 2F) or fold changes (Fig. 2G). The set of primary induced targets enriched for genes involved in cell-cycle progression, DNA, RNA, and protein biosynthesis (Supplementary Fig. S4C; Supplementary Table S2), concordant with the observations in multiple models and with the general growth-promoting activity of MYC (8, 10, 21).

To further validate the direct regulation of the primary target genes identified in the tet-MYC model, we used a different switchable KI mouse model that expresses elevated levels of MYC-ER^{TAM} in the liver (Pellegrinet and colleagues; manuscript in preparation). RNA-seq analysis following short-term activation (6 hours) of MYC-ER^{TAM} revealed consistent responses of the primary MYC-induced and repressed mRNAs previously defined in the T→Toff transition (categories 2, 3 and 5, 6, respectively; Fig. 2H). Hence, switching MYC off in tumors and activating it in the normal liver revealed conservation of the direct transcriptional responses in these two different states.

Altogether, most of the genes that were deregulated during tumorigenesis showed no direct dependency upon MYC in tumors, even though most of those genes are also bound by MYC in their promoters (see below). Thus, more than DNA binding, RNA-seq analysis following tet-MYC shutdown allowed narrowing down on those genes that are primarily regulated by MYC (Supplementary Table S1), and are thus the most likely to be its direct effectors in tumor progression and maintenance. These data are also consistent with the notion that besides MYC-activated genes, repressed genes may be as important in tumorigenesis (8, 30). Hereafter, we present data that directly address this notion.

Primary repression is selectively compromised in MYC-VD–induced tumors

To address the transcriptional activity of MYC-VD, we established RNA-seq profiles in the corresponding tumors and identified DEGs relative to control liver samples. Hierarchical clustering only partially discriminated WT- from VD-induced tumors (hereafter T and Tvd; Fig. 3A), in line with the similar expression profiles of those tumor populations (Fig. 3B). Consistent with this

Figure 1.

tet-MYC-VD is impaired in liver tumor induction compared with tet-MYC-WT. A, representative photos of double-transgenic tet-MYC/LAPtTA mice upon tet-MYC induction *in utero,* or single-transgenic tet-MYC control mice, showing the increased abdominal size in male and female double-transgenic mice by the age of 6 weeks. B, Kaplan–Meier survival curve of tet-MYC-WT (orange) or tet-MYC-VD (green) overexpressing, or control (wild-type or single-transgenic, black) mice. Mice were euthanized and scored when moribund. The median survival was 5 weeks for tet-MYC-WT and 13 weeks for tet-MYC-VD–expressing mice. Significance was assessed using the log-rank test. C, representative photo of a tet-MYC-WT–overexpressing liver containing multiple tumor nodules. D, mRNA and Western blot analyses of human *MYC* mRNA (= transgene) and mouse/human MYC protein expression in control liver and tet-MYC-WT tumor samples. For Western blot analyses, the MYC antibody Y69 was used. It recognizes MYC of mouse and human origin. E, representative immunohistochemical stainings of control, tet-MYC-WT, and tet-MYC-VD samples, using antibodies targeting MYC or E-cadherin. F, human *MYC* mRNA levels in control (C) livers or tet-MYC-WT tumors before (T) or after (16 hours; Toff) doxycycline treatment were assessed by qRT-PCR. For Western blot analyses, the MYC antibody Y69 was used (see C). G, photos of one tet-MYC-WT–expressing mouse at the age of 6 weeks before switching off tet-MYC transgene expression, displaying strong abdominal swelling (left). Providing doxycycline food led to rapid regression of the tumors, as observable on the photos taken after 1 (middle) and 3.5 weeks (right) of treatment. H, liver weight (in grams, g) of control (C), tet-MYC-WT (T), or tet-MYC-VD (Tvd) overexpressing mice on the day of euthanasia. Significance was assessed with the Student *t* test and *P* values are displayed in the figure or as follows: T vs. C, 4.6×10^{-37}; Tvd vs. C, 2.3×10^{-37}. I, qRT-PCR analyses of human *MYC* mRNA levels in tumors (T or Tvd) or control livers. The numbers in brackets originate from independent replicates per genotype. Significance was assessed using the Student *t* test. J and K, primary fHBs were purified from embryos on day E18.5 using anti-E-cadherin antibodies. Upon short-term *in vitro* culture, fHBs were infected with sh*p53*, MYC, and, where indicated, RAS^{G12V}. J, cells were plated in triplicates in semisolid medium [50% methylcellulose (v/v)] and cultured for 7 days. Data were normalized to plated cell numbers, measured by absorbance values of the MTT assay performed on parallel cultures 24 hours after plating. Significance was assessed with the Student *t* test. K, fHBs were injected into CD1-nude mice and tumor volumes were determined on the indicated days. The inset shows the corresponding tumors on day 14.

Published OnlineFirst April 13, 2016; DOI: 10.1158/0008-5472.CAN-16-0316

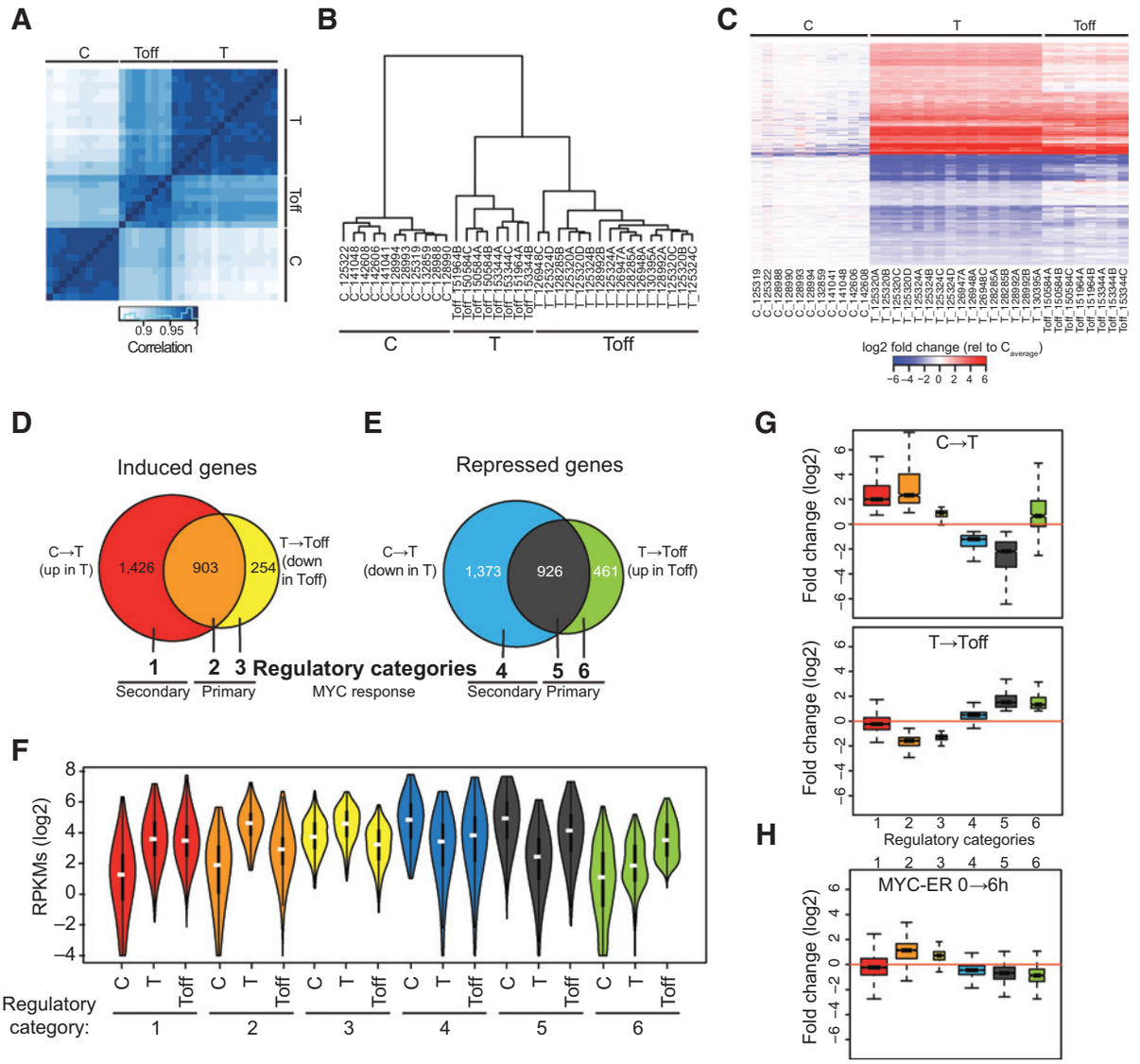

Figure 2.

RNA-seq analyses after short-term MYC inactivation identify MYC-dependent and MYC-independent DEG categories. A, hierarchical clustering (Spearman correlation, method "complete") of RNA sequencing results of control liver samples (C, $n = 11$) and tet-MYC tumors before (T, $n = 16$) or after (Toff, $n = 8$) short-term inactivation (16 hours) of the exogenous tet-MYC transgene. Samples originate from separate tumor nodules from a total of 11 C, 7 T, or 3 Toff mice. B, cluster dendrogram of the hierarchical clustering (see A). Sample identification numbers of the biologic replicates are shown, including a unique six-digit code and the nodule name (defined by letters, e.g., A–D). C, heatmap showing DEGs (from C→T) of C, T, and Toff samples. Shown are mRNA expression fold changes relative to the average expression among all control liver replicates. D and E, Venn diagrams of MYC-induced (D) and repressed (E) genes. DEGs were calculated comparing tumors with control samples (C→T), or tumors after to before tet-MYC inactivation (T→Toff), the latter defining the primary, MYC-dependent DEG categories. The regulatory categories defined here will be used throughout this work. F, violin plots depicting the expression levels (RPKM, log2) of genes belonging to primary and secondary regulatory categories (see D and E). G, box plots showing the expression fold changes (log2) of the different regulatory categories, as indicated below the graphs. Comparisons were done at the control to tumor transition (C→T, top), or the transition from tumors before to after Tet-MYC inactivation (T→Toff, bottom). H, box plot displaying expression fold changes (log2) of MYC target genes (identified in the tet-MYC mouse model) in liver samples of adult mice expressing a TAM-inducible MYC-ER transgene. Samples were taken 6 hours after TAM injection.

finding, either up- or downregulated genes in the C→T and C→Tvd transitions were largely overlapping (Fig. 3C). Yet, an important difference emerged when distinguishing among the different regulatory modes previously identified on the basis of the shut-off of tet-MYC-WT. In particular, secondary response genes were similarly deregulated in C→T and C→Tvd, regardless of whether they were induced or repressed (Fig 3D, i and ii). The same was true for the primary MYC-induced genes (Fig 3D, iii), confirming that MYC-VD is as effective as WT in transcriptional activation (18). Instead, primary MYC-repressed genes showed weaker downregulation in C→Tvd relative to C→T (Fig 3D, iv): among these, 285 genes were repressed with a 2-fold lower

Published OnlineFirst April 13, 2016; DOI: 10.1158/0008-5472.CAN-16-0316

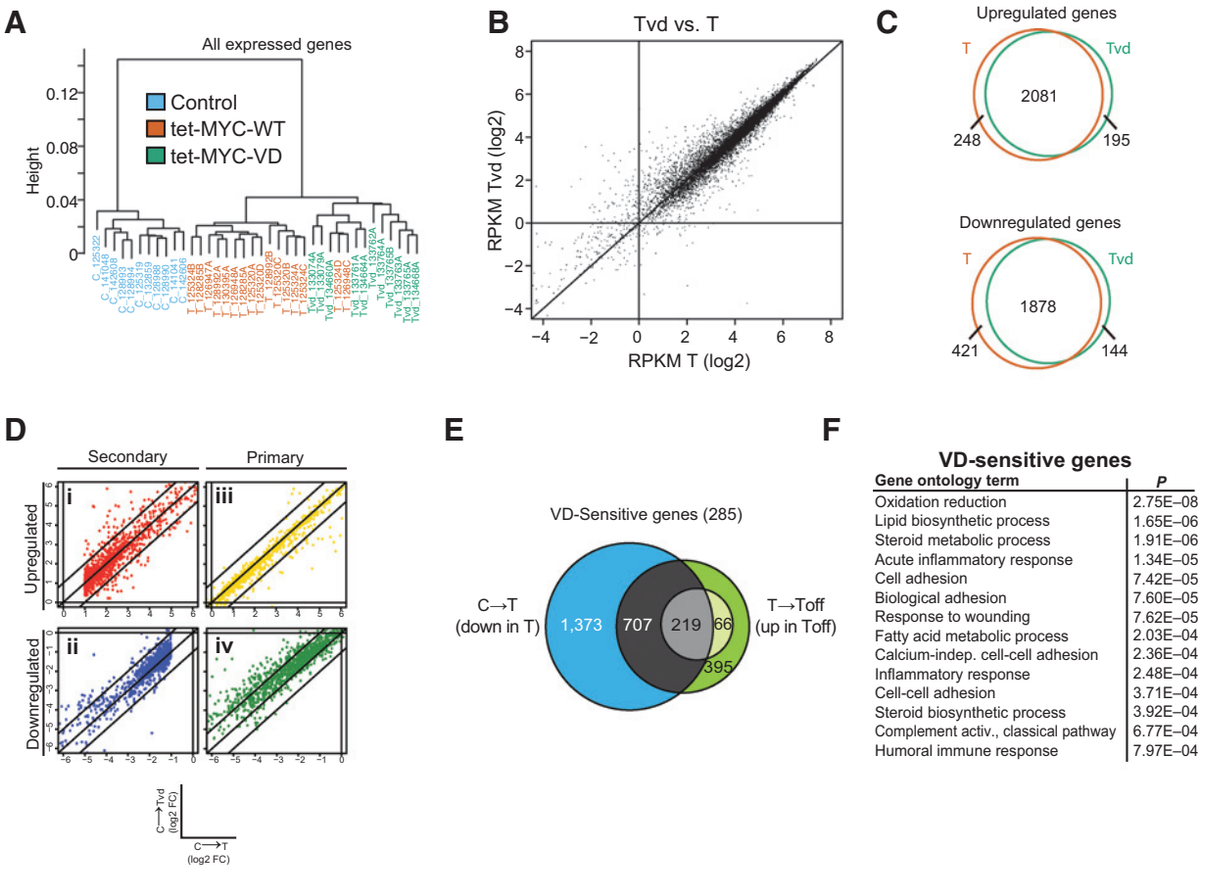

Figure 3.
Tet-MYC-VD is deficient in MYC-dependent gene repression. A, hierarchical clustering (Spearman correlation, method "complete") of RNA sequencing results of control liver samples (C, $n = 11$, blue), tet-MYC-WT (T, $n = 16$, orange), and tet-MYC-VD tumors (Tvd, $n = 11$, green). Sample identification numbers of the biologic replicates are shown, including a unique six-digit code and the nodule name (defined by letters, e.g., A–D). B, scatterplot showing RPKM expression values (log2) in tet-MYC-WT (T, *x*-axis) and tet-MYC-VD (Tvd, *y*-axis) samples. Shown is the average expression across the biologic replicates described in A. C, Venn diagrams displaying the overlap of DEGs in T or Tvd tumors compared with control livers, subdivided into up- (top) and downregulated (bottom) genes. D, scatterplots comparing fold change expression values (log2) of the C→T (*x*-axis) or the C→Tvd (*y*-axis) transitions. Shown are induced (top) or repressed (bottom) DEGs, separated into primary (iii, iv) and secondary (i, ii) MYC-responsive genes. E, Venn diagram showing the numbers of MIZ1-dependent genes belonging to the primary MYC-responsive DEGs (for details, see Supplementary Table S3). F, gene ontology analyses of MIZ1-dependent downregulated DEGs were performed using the DAVID online tool.

efficiency in MYC-VD relative to MYC-WT tumors (Fig. 3E; Supplementary Table S3), enriching for functional categories including cell adhesion/response to wounding (Fig. 3F), as previously reported in different cellular compartments (18, 31).

Genomic MYC-binding profiles are not predictive of MYC-dependent regulation

MYC associates with active promoters and enhancers in a highly promiscuous manner and up- or downregulates large, yet discrete sets of genes, although no general rules have yet emerged concerning the relationship between DNA binding and gene regulation (8). To address this issue in our model, we used ChIP-seq technology to determine the chromatin-binding profiles of MYC, RNA polymerase II (RNAPII), and the active histone marks H3K4me3 and H3K27ac. Focusing on annotated promoter regions revealed a tight correlation between the presence of RNAPII, H3K4me3, and H3K27ac (in either C, T, or Toff samples) and MYC binding in T, while promoters lacking those features remained unbound (Supplementary Fig. S5A–S5D). Most importantly, active promoter marks pre-existed in C and were retained following MYC elimination in Toff. Thus, consistent with other studies, overexpressed MYC in T widely associated with already active promoters while inactive promoters remained unbound (3–5, 7, 8).

MYC-binding profiles did not allow distinguishing primary from secondary MYC-responsive genes, whether considering the presence of a MYC peak at the promoter (Supplementary Fig. S5E), its localization relative to the TSS (Supplementary Fig. S5F), or binding intensities in control liver or tumors (Fig. 4A). Remarkably, relative to nonregulated genes, primary repressed genes (categories 5, 6) were less frequently and more weakly bound, and showed a lower frequency of E-boxes around their TSS, while the opposite was true for primary induced genes (categories 2, 3; Fig. 4A and Supplementary Fig. S5G). These features were confirmed among MYC-ER–responsive genes in fibroblasts (Supplementary Fig. S5H; ref. 5). In tumors, overexpressed MYC

Published OnlineFirst April 13, 2016; DOI: 10.1158/0008-5472.CAN-16-0316

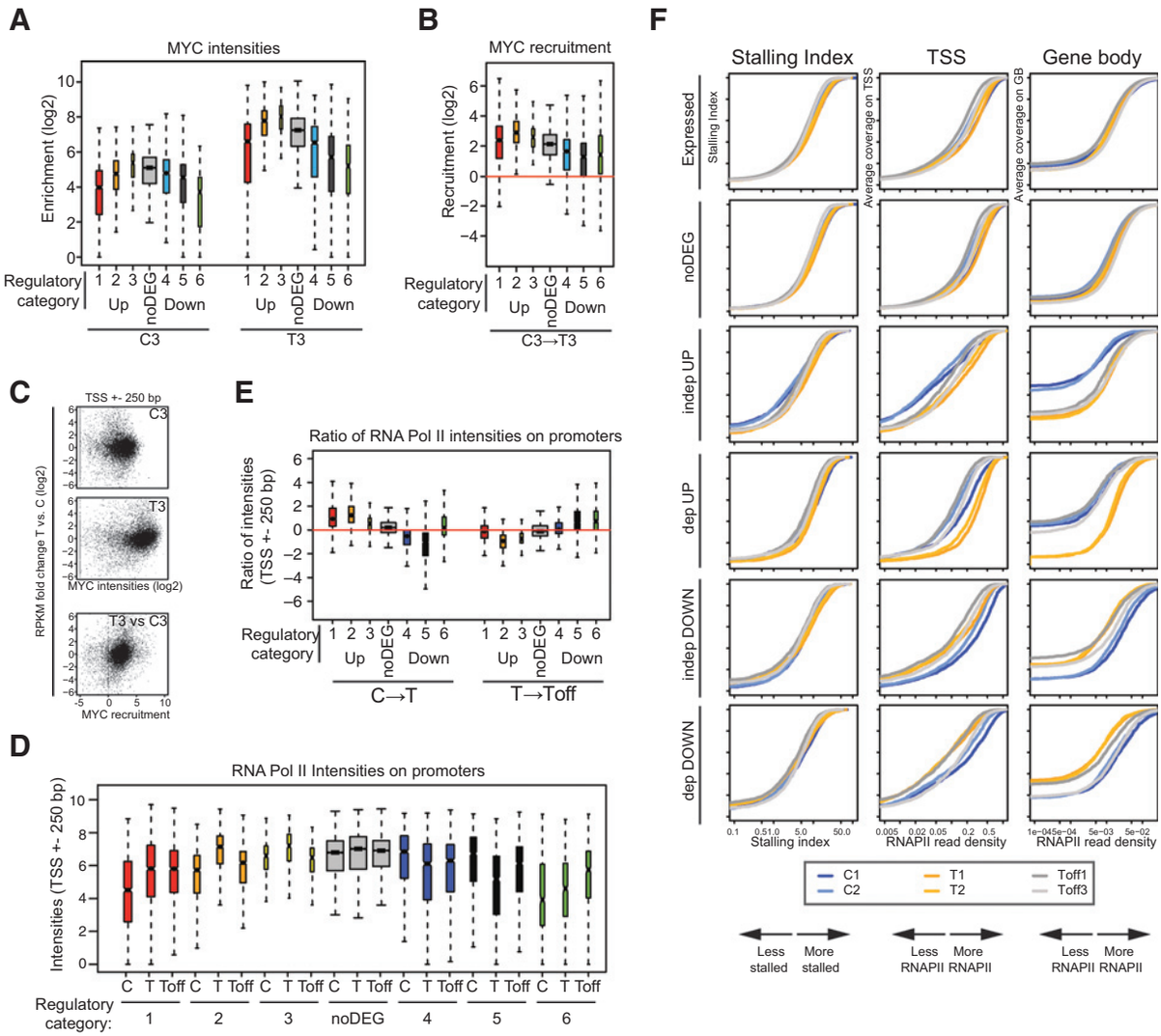

Figure 4.

Genome-wide MYC binding alone does not discriminate between primary and secondary MYC-target genes, but changes in RNA Pol II activity corresponds to the DEG categories. A, MYC ChIP-seq intensities on promoters (TSS ± 250 bp) in one exemplary control liver (C3) and tumor (T3), respectively. Genes are separated into the regulatory categories as described in Fig. 2D and E. The category "noDEG" contains genes that do not significantly change their expression at the C→T transition. The width of the boxes is proportional to the numbers of genes contained in each category. B, ratio between MYC intensities (for details, see A) in the different DEG categories. C, MYC intensities on promoters (TSS ± 250 bp) in C3 (top), T3 (middle), or their ratio (bottom) relative to fold expression of the respective gene at the C→T transition (log2). D, RNA Pol II intensities on promoters (TSS ± 250 bp) in control liver (C2) and tet-MYC tumors before (T2) and after (Toff3) tet-MYC shutdown for 16 hours. Genes were classified as described in A. E, ratio between RNA Pol II intensities on promoters (for details, see D) in the different DEG categories described above. F, RNA Pol II read densities on the TSS (middle; TSS ± 300 bp) and gene bodies [right; TSS + 300 bp to TES (transcriptional end site)] and their ratio (left), termed stalling index (33), was calculated for all expressed genes or for the DEG categories as indicated, independently of the presence or absence of RNA Pol II peaks at the corresponding promoter. The three measures are displayed for 2 C (blue), 2 T (orange), and 2 Toff (gray) samples.

associated with active promoters in a widespread manner, but increases in binding neither discriminated MYC-dependent from -independent transcriptional responses (Fig. 4B), nor correlated with the extent of changes in mRNA levels (Fig. 4C). Furthermore, neither MYC-binding nor recruitment to enhancers (determined by nearest-neighbor analyses) in C or T discriminated primary from secondary MYC target genes (Supplementary Fig. S5I and S5J). Taken together, no simple rule could be drawn that would link promoter/enhancer association by MYC with either primary or secondary gene regulation.

MYC influences promoter-loading of RNA Pol II at both activated and repressed loci

MYC was suggested to regulate global RNA Pol II activity at the elongation step (15), although other observations were inconsistent with the generality of this effect (5, 8) and effects have also been reported at the RNA Pol II loading step (14, 32). RNA Pol II–binding intensities in the promoter regions of expressed genes correlated well within C or T replicates, while larger variations occurred during the C→T transition (Supplementary Fig. S6A). Most importantly, up- or downregulation of gene expression was

Published OnlineFirst April 13, 2016; DOI: 10.1158/0008-5472.CAN-16-0316

paralleled by equivalent changes in RNA Pol II binding at promoters (Supplementary Fig. S6B). In particular, while during the C→T transition, either primary or secondary genes (classes 2/5 and 1/4, respectively) showed similar variations in Pol II binding (Fig. 4E), only primary MYC-dependent genes (classes 2,3/5,6) were affected during the T→Toff transition (Fig. 4D and E). Thus, MYC influences RNA Pol II loading on either activated or repressed genes.

Transcription can be regulated at all steps of the RNA Pol II life cycle, including loading, pausing, and elongation. To investigate the relative contribution of these steps in our experimental system, we calculated the RNA Pol II occupancy on promoters and gene bodies, as well as their ratio, or stalling index (also termed traveling ratio; refs. 15, 33) for the different regulatory groups. Computing these values for the different regulatory classes (Fig. 4F) showed consistent changes in Pol II abundance not only on promoters, as mentioned above, but also on gene bodies. However, stalling indices were not consistently affected in any of the regulatory categories, confirming this measure alone is insufficient in assessing RNA Pol II dynamics (5, 34). Altogether, whether regulated by MYC in a primary or secondary manner, activated and repressed genes showed generally consistent changes in Pol II loading and elongation. Further studies will be required to elucidate the contribution of each regulatory step to MYC activity.

Discussion

The addiction of tumors to oncogenes such as *c-MYC* (2) indicates that deregulated oncogenic signaling is continuously required for tumor maintenance. Identifying the downstream effectors of driving oncogenes in specific tumor types is thus an important means to narrow down on possible therapeutic targets. Here, we profiled transcriptional responses in liver carcinomas driven by a tetracycline-repressible tet-MYC transgene (19, 22). A previous study based on an analogous model reported profiles obtained 3 days after MYC shut-off (35): at this stage, however, a number of indirect effects are likely to become predominant, including apoptosis or differentiation into hepatocytes and biliary cells (23). Using short-term inactivation of the transgene in tumors (16 hours), we showed that MYC was directly required for either activation or repression of distinct groups of genes (each over 1,000 genes). These MYC-dependent genes represented close to half of all those deregulated in tumors relative to normal tissue. This difference was expected, as tumor transcriptomes are shaped by a series of indirect effects, such as the deregulation of other transcription factors, RNA-regulatory proteins, or miRNAs, as well as changes in cellular metabolism, differentiation state, and others (8, 10, 21). Thus, most importantly, our data allowed us to discriminate between primary MYC-regulated targets and a plethora of secondary, indirect changes in gene expression.

Besides tet-MYC, we used tet-MYC-VD transgenic mice, encoding a mutant defective in binding to the corepressor MIZ1. As in other tissues (19, 24), tet-MYC-VD in the liver showed significantly reduced tumorigenic potential relative to wild-type MYC. Expression profiling of MYC-VD–driven tumors showed a selective impairment in the downregulation of a subset of the primary MYC-repressed genes identified upon tet-MYC shut down. Hence, MIZ1-dependent repression plays an important role in MYC-induced liver tumorigenesis. In line with the fact that MYC-repressed transcriptional programs appear to be largely tissue-specific, the requirement for the MYC-MIZ1 interaction appears to differ among the tumor types studied so far, including suppression of TGFβ-mediated senescence in T-cell lymphomas (19), maintenance of stemness in medulloblastoma (24) and, possibly related to the latter, tumor initiation in the liver (this work).

Altogether, the data presented in this and previous work (5, 6, 8) show that only a fraction of the MYC-bound genes are deregulated during tumorigenesis, with molecular determinants that largely remain to be understood (8). In turn, as shown here, only about half of these deregulated genes (whether activated or repressed) show dependency upon MYC in tumors and may thus represent direct regulatory targets: others may be deregulated through indirect mechanisms or, alternatively, may be expressed in infiltrating cells, such as lymphocytes or leukocytes, as also suggested by gene ontologies (Supplementary Fig. S4C). Most noteworthy in this regard, MYC may directly modulate the expression of molecules that control the recruitment/activation of immune cells: CD47 and PD-L1 (CD274), for example, were recently reported to be downregulated upon tet-MYC inactivation in either liver tumors or lymphomas, contributing to tumor clearance in the latter (36). The generality of this mechanism remains to be evaluated, however, as CD47 and CD274 were slightly upregulated upon MYC inactivation in our liver model (Supplementary Table S1).

Consistent with previous studies, MYC-activated genes were particularly enriched for molecules involved in cell-cycle progression, proliferation, DNA and RNA biology (Supplementary Fig. S4C; Supplementary Table S2; refs. 8, 21). Functional screens will be instrumental in determining which of these direct regulatory targets are essential effectors of MYC in tumor maintenance, and may thus become the focus of future therapeutic development.

Disclosure of Potential Conflicts of Interest

No conflicts of interest were disclosed by the authors.

Authors' Contributions

Conception and design: T.R. Kress, B. Amati

Development of methodology: T.R. Kress, L. Pellegrinet, M. Ravà

Acquisition of data (provided animals, acquired and managed patients, provided facilities, etc.): T.R. Kress, P. Pellanda, L. Pellegrinet, P. Nicoli, M. Doni, S. Bianchi, L. Rotta, T. Capra, A. Verrecchia, T.D. Littlewood

Analysis and interpretation of data (e.g., statistical analysis, biostatistics, computational analysis): T.R. Kress, V. Bianchi, C. Recordati, E. Radaelli, G.I. Evan, B. Amati

Writing, review, and/or revision of the manuscript: T.R. Kress, L. Pellegrinet, G.I. Evan, B. Amati

Administrative, technical, or material support (i.e., reporting or organizing data, constructing databases): M. Doni, S. Bianchi, L. Rotta, T. Capra, B. Amati

Study supervision: T.D. Littlewood, B. Amati

Acknowledgments

The authors thank Martin Eilers (Theodor Boveri Institute, Würzburg, Germany) for the tet-MYC-WT and tet-MYC V394D mice, Mattia Pelizzola, Stefano de Pretis, Marco Morelli, and Vera Pendino for discussion and advice, the mouse facility of the IFOM-IEO campus for help with maintenance of the mouse colonies, and Federica Pisati for tissue embedding.

Grant Support

This work was supported by grants from the European Community's Seventh Framework Programme (MODHEP consortium, grant agreement no. 259743), the European Research Council (no. 268671), the Italian Health Ministry (RF-2011-02346976), and the Italian Association for Cancer Research (AIRC, no.

Published OnlineFirst April 13, 2016; DOI: 10.1158/0008-5472.CAN-16-0316

13182 to B. Amati). In the initial phase of this study, T.R. Kress was supported by the Structured International Post Doc program of the European School of Molecular Medicine.

The costs of publication of this article were defrayed in part by the payment of page charges. This article must therefore be hereby marked advertisement in accordance with 18 U.S.C. Section 1734 solely to indicate this fact.

Received February 1, 2016; accepted February 11, 2016; published OnlineFirst April 13, 2016.

References

1. Vita M, Henriksson M. The Myc oncoprotein as a therapeutic target for human cancer. Semin Cancer Biol 2006;16:318–30.
2. Gabay M, Li Y, Felsher DW. MYC activation is a hallmark of cancer initiation and maintenance. Cold Spring Harb Perspect Med 2014;4:pii: a014241.
3. Lin CY, Loven J, Rahl PB, Paranal RM, Burge CB, Bradner JE, et al. Transcriptional amplification in tumor cells with elevated c-Myc. Cell 2012;151:56–67.
4. Nie Z, Hu G, Wei G, Cui K, Yamane A, Resch W, et al. c-Myc is a universal amplifier of expressed genes in lymphocytes and embryonic stem cells. Cell 2012;151:68–79.
5. Sabo A, Kress TR, Pelizzola M, de Pretis S, Gorski MM, Tesi A, et al. Selective transcriptional regulation by Myc in cellular growth control and lymphomagenesis. Nature 2014;511:488–92.
6. Walz S, Lorenzin F, Morton J, Wiese KE, von Eyss B, Herold S, et al. Activation and repression by oncogenic MYC shape tumour-specific gene expression profiles. Nature 2014;511:483–7.
7. Guo J, Li T, Schipper J, Nilson KA, Fordjour FK, Cooper JJ, et al. Sequence specificity incompletely defines the genome-wide occupancy of Myc. Genome Biol 2014;15:482.
8. Kress TR, Sabo A, Amati B. MYC: connecting selective transcriptional control to global RNA production. Nat Rev Cancer 2015;15:593–607.
9. Smith AP, Verrecchia A, Faga G, Doni M, Perna D, Martinato F, et al. A positive role for Myc in TGFbeta-induced Snail transcription and epithelial-to-mesenchymal transition. Oncogene 2009;28:422–30.
10. Eilers M, Eisenman RN. Myc's broad reach. Genes Dev 2008;22:2755–66.
11. Amati B, Brooks MW, Levy N, Littlewood TD, Evan GI, Land H. Oncogenic activity of the c-Myc protein requires dimerization with Max. Cell 1993; 72:233–45.
12. Kato GJ, Barrett J, Villa-Garcia M, Dang CV. An amino-terminal c-myc domain required for neoplastic transformation activates transcription. Mol Cell Biol 1990;10:5914–20.
13. Tu WB, Helander S, Pilstal R, Hickman KA, Lourenco C, Jurisica I, et al. Myc and its interactors take shape. Biochim Biophys Acta 2015;1849:469–83.
14. Bouchard C, Marquardt J, Bras A, Medema RH, Eilers M. Myc-induced proliferation and transformation require Akt-mediated phosphorylation of FoxO proteins. EMBO J 2004;23:2830–40.
15. Rahl PB, Lin CY, Seila AC, Flynn RA, McCuine S, Burge CB, et al. c-Myc regulates transcriptional pause release. Cell 2010;141:432–45.
16. Dunn S, Cowling VH. Myc and mRNA capping. Biochim Biophys Acta 2015;1849:501–5.
17. Lee LA, Dolde C, Barrett J, Wu CS, Dang CV. A link between c-Myc-mediated transcriptional repression and neoplastic transformation. J Clin Invest 1996;97:1687–95.
18. Wiese KE, Haikala HM, von Eyss B, Wolf E, Esnault C, Rosenwald A, et al. Repression of SRF target genes is critical for Myc-dependent apoptosis of epithelial cells. EMBO J 2015;34:1554–71.
19. van Riggelen J, Muller J, Otto T, Beuger V, Yetil A, Choi PS, et al. The interaction between Myc and Miz1 is required to antagonize TGFbeta-dependent autocrine signaling during lymphoma formation and maintenance. Genes Dev 2010;24:1281–94.
20. Vo BT, Wolf E, Kawauchi D, Gebhardt A, Rehg JE, Finkelstein D, et al. The interaction of Myc with Miz1 defines medulloblastoma subgroup identity. Cancer Cell 2016;29:5–16.
21. Stine ZE, Walton ZE, Altman BJ, Hsieh AL, Dang CV. MYC, metabolism, and Cancer. Cancer Discov 2015;5:1024–39.
22. Beer S, Zetterberg A, Ihrie RA, McTaggart RA, Yang Q, Bradon N, et al. Developmental context determines latency of MYC-induced tumorigenesis. PLoS Biol 2004;2:e332.
23. Shachaf CM, Kopelman AM, Arvanitis C, Karlsson A, Beer S, Mandl S, et al. MYC inactivation uncovers pluripotent differentiation and tumour dormancy in hepatocellular cancer. Nature 2004;431:1112–7.
24. Vo BT, Wolf E, Kawauchi D, Gebhardt A, Rehg JE, Finkelstein D, et al. The interaction of Myc with Miz1 defines medulloblastoma subgroup identity. Cancer Cell 2016;29:5–16.
25. Perna D, Faga G, Verrecchia A, Gorski MM, Barozzi I, Narang V, et al. Genome-wide mapping of Myc binding and gene regulation in serum-stimulated fibroblasts. Oncogene 2012;31:1695–709.
26. Trumpp A, Refaeli Y, Oskarsson T, Gasser S, Murphy M, Martin GR, et al. c-Myc regulates mammalian body size by controlling cell number but not cell size. Nature 2001;414:768–73.
27. Cairo S, Armengol C, De Reynies A, Wei Y, Thomas E, Renard CA, et al. Hepatic stem-like phenotype and interplay of Wnt/beta-catenin and Myc signaling in aggressive childhood liver cancer. Cancer Cell 2008; 14:471–84.
28. Zender L, Xue W, Cordon-Cardo C, Hannon GJ, Lucito R, Powers S, et al. Generation and analysis of genetically defined liver carcinomas derived from bipotential liver progenitors. Cold Spring Harb Symp Quant Biol 2005;70:251–61.
29. Herold S, Wanzel M, Beuger V, Frohme C, Beul D, Hillukkala T, et al. Negative regulation of the mammalian UV response by Myc through association with Miz-1. Mol Cell 2002;10:509–21.
30. Herkert B, Eilers M. Transcriptional repression: the dark side of myc. Genes Cancer 2010;1:580–6.
31. Gebhardt A, Frye M, Herold S, Benitah SA, Braun K, Samans B, et al. Myc regulates keratinocyte adhesion and differentiation via complex formation with Miz1. J Cell Biol 2006;172:139–49.
32. Martinato F, Cesaroni M, Amati B, Guccione E. Analysis of Myc-induced histone modifications on target chromatin. PLoS One 2008;3: e3650.
33. Zeitlinger J, Stark A, Kellis M, Hong JW, Nechaev S, Adelman K, et al. RNA polymerase stalling at developmental control genes in the Drosophila melanogaster embryo. Nat Genet 2007;39:1512–6.
34. Jonkers I, Lis JT. Getting up to speed with transcription elongation by RNA polymerase II. Nat Rev Mol Cell Biol 2015;16:167–77.
35. Hu S, Balakrishnan A, Bok RA, Anderton B, Larson PE, Nelson SJ, et al. 13C-pyruvate imaging reveals alterations in glycolysis that precede c-Myc-induced tumor formation and regression. Cell Metab 2011;14: 131–42.
36. Casey SC, Tong L, Li Y, Do R, Walz S, Fitzgerald KN, et al. MYC regulates the antitumor immune response through CD47 and PD-L1. Science. 2016 Mar 10. [Epub ahead of print].

Published OnlineFirst April 13, 2016; DOI: 10.1158/0008-5472.CAN-16-0316

Cancer Research
The Journal of Cancer Research (1916–1930) | The American Journal of Cancer (1931–1940)

AACR American Association for Cancer Research

Identification of MYC-Dependent Transcriptional Programs in Oncogene-Addicted Liver Tumors

Theresia R. Kress, Paola Pellanda, Luca Pellegrinet, et al.

Cancer Res 2016;76:3463-3472. Published OnlineFirst April 13, 2016.